

1 **Spatiotemporal quantification of key environmental changes in Stok and**
2 **Kang Yatze regions of Ladakh Himalaya, India**

3 Mohd Soheb^{a*}, Alagappan Ramanathan^a, Anshuman Bhardwaj^b, Lydia Sam^b

4 ^a*School of Environmental Sciences, Jawaharlal Nehru University, New Delhi, India*

5 ^b*School of Geosciences, University of Aberdeen, King's College, Aberdeen AB24 3UE, UK*

6

7 Corresponding author: sohaib.achaa@gmail.com

8

9

10

11

12

13

14

15

16

17

18

19

20

21

22

23

24

25

26

27 **Spatiotemporal quantification of key environmental changes in Stok and**
28 **Kang Yatze regions of Ladakh Himalaya, India**

29

30 **Abstract:**

31 Tourism fuelled economic transformation of Ladakh region is bringing a change in
32 demography and livelihood preferences leading to increased exploitation of scarce natural
33 resources. In addition to the nerve centre of tourism-related activities (Leh city), rural
34 hinterlands of Ladakh are also witnessing a stark transformation in land and resource use
35 patterns. In this study we quantified and assessed the changes in key environmental parameters
36 of rural Ladakh between 1969 and 2020. We observed a decrease in glacier area, glacier volume
37 and vegetation cover by ~19%, 13% and 14%, whereas built-up and lake area increased by
38 ~238% and 122%, respectively. Simultaneously, local population of the region doubled while
39 tourism footprint increased by ~620 folds. The study highlights the environmental changes
40 happening at a higher rate in rural regions around Leh city. Therefore, need of the hour is to
41 recognise the disruptive changes being brought in the traditional way of life and to devise
42 strategies to reorient the development paradigm towards sustainable resource use and
43 management.

44

45 **Keywords:** Ladakh, tourism, environment, climate change, glacier, Himalaya.

46

47

48

49

50

51

52

53

54

55

56

57

58

59 **1. Introduction**

60 Mountainous regions in Himalaya face various sustainability challenges due to climate,
61 geopolitical, economic, and societal transformations, which affect environment, water
62 resources and demography of the land (Bhardwaj et al. 2019). Some of the major factors for
63 such transformations are the climate change (Sam et al. 2019), booming tourism industry,
64 international conflicts, rapid urbanisation and migration. These factors will have both positive
65 and negative impact on the environment and society. Positive impacts comprise of warmer
66 climate more conducive to habitation, improvement in living standards and economy,
67 agricultural growth, and improved connectivity, among others. However, the negative impacts
68 are often long-lasting, irreversible, and more damaging, and consist of excessive stress on the
69 environment, unplanned development, exploitation of natural resources, and pollution, among
70 others. Policy design and implementation is challenging in mountains, because usually these
71 regions have been of marginal concern due to lesser population, and therefore often ignored in
72 development priorities (Messerli and Ives 1997; Geneletti and Dawa 2009). Environmental
73 fragility and tourism seasonality of mountain regions further add to the issues hindering
74 systematic and integrated developments (Buckley et al. 1999; Arrowsmith and Inbakaran 2002;
75 Geneletti and Dawa 2009). Moreover, mountain areas often mark international borders for
76 many countries and thus, hold political sensitivity in terms of major policy changes (Nepal and
77 Chipeniuk 2005). With increasing globalisation and political stability in majority of the world,
78 mountain tourism has developed with an accelerated pace in the past several decades (Price
79 1992; Moss and Godde 1999). However, such tourism has led to unprecedented growing
80 environmental concerns in developed (Draper, 2000) and developing countries alike (Stevens,
81 2003, Buntaine et al., 2006).

82 One of such mountainous regions is Ladakh which used to be a restricted land for the outside
83 world due to its geo-strategic sensitivity (Bray, 1991; Warikoo et al., 2020) and tribal

84 population (Smith, 2012). However, the government of India opened the region for tourism in
85 1974 (Bray, 1991), which marked the beginning of a new era for Ladakh. As per the data
86 available from the Leh tourist office, 8,608 Indian and 16,256 foreign tourists visited Ladakh
87 in 1988 (Bray, 1991). Thus, tourism emerged as the prime revenue generator for the region and
88 opened new income sources for guesthouses and hotels, local shops, and guided tours and
89 travels (Bray, 1991; Nüsser, et al., 2019a,b; Müller et al., 2020). However, the initial economic
90 benefits of tourism had been concentrated in the Indus valley, disproportionately benefitting
91 mainly non-Ladakhis (Michaud 1991). With improvements in connectivity and
92 communication, this scenario has evolved in the past two decades as the number of visitors
93 increased many folds over last few decades from a few hundred in 1974 to more than 300,000
94 visitors in 2019 from every corner of the world (Muller et al., 2020). Agriculture used to be the
95 primary sector for the local economy but today it is replaced by tertiary sector (especially
96 tourism) (Dame et al., 2019; Muller et al., 2020). Leh, which is the capital city of Ladakh, has
97 now become one of the most visited cities in high-Himalayan Mountains. The recent decision
98 to develop Ladakh as a Union Territory of India has cleared the path for more rapid urbanisation
99 and development of the region in coming years.

100 While rapid urbanisation of Leh city has recently been investigated from a remote sensing
101 perspective (Dame et al., 2019, Müller et al., 2020), the effects are still unknown for the rural
102 areas around Stok and Kang Yatze range. As mentioned above, such regions along the Indus
103 valley have been the target of this tourism-led changes in Ladakh (Michaud 1991; Nüsser et
104 al., 2012). Thus, for these regions, it is particularly important to quantify the changes in several
105 of the key environmental parameters such as glaciers, vegetation, water, and built-up, between
106 1969 and 2020, to understand the long-term impacts of tourism and demographic changes on
107 high-mountain catchments. In this study we are trying to understand and document the major
108 land cover changes happened in the parts of rural Ladakh for the past 50 years (1969-2020).

109 The main objectives of this research are: (1) to perform temporal mapping of glaciers,
110 vegetation, water, and build-up in Stok and Kang Yatze regions of Ladakh Himalaya; (2) to
111 quantify spatiotemporal changes in the mapped parameters; and (3) to use climate,
112 demography, and other ancillary datasets for further assessing the quantified changes.

113 **2. Study area**

114 In this study, two different adjacent regions (Stok and Kang Yatze region) with various
115 glaciers, build-up, vegetation, and population settings were selected from Ladakh, India (Figure
116 1) to understand the changes occurred due to climate change, tourism, and urbanisation during
117 past five decades. The geographic extent of the study area lies within latitude and longitude of
118 33.3° to 34.3° N and 77.1° to 78.1° E, respectively. It covers a vast area around Stok and Kang
119 Yatze regions extending from 3000 to 6400m a.s.l in the northern Zaskar range, Ladakh, India.
120 The region of interest consists of 15 villages of various sizes with population ranging from 128
121 - 5,565 individuals (Census 2011). Most of these villages are entirely dependent on the glacier
122 and snow meltwater for irrigation and domestic use. Stok and Kang Yatze regions house 30
123 and 106 glaciers of various sizes ranging from 0.01 to 5 km², with larger glaciers (>3 km²)
124 entirely concentrated in Kang Yatze region. In 2019 the total glacierised area was around 89
125 km², equivalent to 3.2% of the study area.

126 Ladakh, the newly formed Union Territory of India, has a unique climate with extremely arid
127 and cold environment. As per the longest in-situ data available from the region headquarter
128 Leh (3500m a.s.l), the long-term yearly mean precipitation sum is <100 mm whereas the mean
129 annual temperature is ~5.6 °C (Nüsser et al., 2012; Soheb et al., 2020). The region is also a hub
130 for wildlife and climbing enthusiasts for its diverse flora fauna and the two famous peaks of
131 Stok (6140m a.s.l.) and Kang Yatze (6400m a.s.l.) summit. Apart from agriculture and service
132 sector, tourism has developed as a major driver of the local economy of the region in the current

133 times (Dame et al., 2019; Müller et al., 2020). Figure 1 presents the study area and the key
134 environmental parameters within the region.

135 **3. Data and methods**

136 In this study, we used freely available multiple datasets from various sources to understand the
137 transformations in key environmental parameters such as vegetation, build-up, glacierised
138 areas, water bodies, and demography (Table 1). The information on multisource datasets used
139 within this study are provided in Table 1. Below we provide descriptions of used datasets and
140 methods for each of the objectives.

141 ***3.1. Glacier mapping***

142 For glacier mapping, Orthorectified level-1T Landsat-Thematic Mapper (TM) and Operational
143 Land Imager (OLI) images (www.earthexplorer.usgs.gov) with minimum (<30%) cloud cover
144 from ablation period (August-September) were used to map the glacierised region of different
145 time periods (1991, 1998, 2010 and 2019). Several robust and established methods to map
146 glaciers are available in literatures e.g. Band ratio approach (Paul et al., 2002, 2015;
147 Racoviteanu et al., 2009; Bhardwaj et al., 2014; Bhardwaj et al., 2015; Schmidt & Nüsser,
148 2017; Smith et al., 2015; Winsvold et al., 2014, 2016), supervised classification methods
149 (Muhammad et al., 2013; Khan et al., 2015; Nagai et al., 2016; Tian et al., 2017; Muhammad
150 2019), and manual delineation method among others.

151 In this study, glacier mapping was carried out by closely following the Global Land Ice
152 Measurements from Space guidelines (Raup et al., 2010). We used the ratio approach between
153 Near Infrared and Shortwave Infrared bands with a threshold of 2.0 ($\text{NIR}/\text{SWIR} > 2 =$
154 ice/snow). A median filter of kernel size 3 x 3 was applied to remove the isolated and small
155 pixels outside the glacier area. The NIR and SWIR band ratio approach is good at
156 distinguishing glacier pixels from water features with similar spectral reflectance values

157 (Racoviteanu et al. 2009; Zhang et al. 2019). Band ratio technique doesn't perform well in
158 shadowed regions therefore additional manual corrections was required (Muhammad and Tian
159 2016). This method is robust and time-efficient for mapping clean glacier (Paul and Kaab,
160 2005; Andreassen et al., 2008) and fortunately the study area only consists of clean glaciers.

161 Multiple high resolution PlanetScope images (www.planet.com) of 29 August 2018 and
162 Google Earth were also used to improve the mapping for the current extent of glaciers. The
163 extent of glaciers in the accumulation zone were kept unchanged throughout the mapping
164 periods because no significant changes is expected in these regions, and also this approach
165 helps in minimising the error in mapping a glacier (Bolch et al., 2010; Bhambri et al., 2013;
166 Garg et al., 2019).

167 Six Corona KH-4A images (www.earthexplorer.usgs.gov) from 30 July 1969, with minimum
168 snow cover, were used to extract the historical extent of glaciers of the study area. Owing to
169 the complex geometry of corona imagery, 12 subsets were made for the study area. All the
170 subsets were separately co-registered following the steps performed by (Bhambri et al., 2011).
171 A projective transformation using ground control points (GCPs) and the Advanced Spaceborne
172 Thermal Emission and Reflection Radiometer Digital Elevation Model (ASTER DEM) was
173 performed followed by a spline adjustment in ArcGIS 10.5. Stable boulders, stupas, historical
174 sites, Monasteries, road junctions and bridges among others were used to collect GCPs. The
175 primary focus of the Corona image rectification was to georectify the glacierised and build-up
176 areas. Digitization of 1969 glacier outlines were manually carried out on the corrected Corona
177 image subsets.

178 ***3.2. Glacier thickness and volume estimation***

179 ASTER DEM from two periods at a temporal gap of atleast 10 years, with no cloud cover over
180 glaciers of the study area, from the ablation time was required to estimate the volume of these

181 ice masses of the study area and see the changes over time. DEM from 2004 and 2020 satisfied
182 the conditions and were chosen for further analysis. The ASTER DEM products (AST14DMO)
183 are created using only orbital ancillary data and without GCPs, therefore small outliers (peaks
184 and sinks) are likely to be present in DEMs. These outliers were removed using the method
185 followed by Shukla and Garg, 2019. Relative horizontal and vertical biases are often present
186 in DEMs derived from different sensors (Nuth and Kaab, 2011). In the present study, we
187 observed a slight shift in the DEMs from the same sensor for the two periods (2004 and 2020).
188 Therefore, the three-dimensional coregistration of the DEMs was required to be performed on
189 stable areas (least error prone regions, e.g., flat valleys, grass lands and farms among others).
190 We followed the coregistration method developed by (Nuth and Kaab, 2011) to minimise the
191 horizontal and vertical biases. The glacierised areas were first removed from the DEMs
192 followed by the areas with a slope between 4-45 degrees, cloud cover, large outliers (elevation
193 difference $>\pm 100\text{m}$) and pixel elevation below 4000m a.s.l. (as no glacier is present in this
194 region below this elevation). The horizontal shift between the reference and slave DEM was
195 corrected significantly. The X and Y shift was reduced from 26.5 and 23.81 m to 4.13 and 3.45
196 m, respectively. However, the vertical biases available in the DEMs were corrected using all
197 ($> 20,000$ pixels) the reliable elevations differences over the stable terrains (Nuth and Kaab,
198 2011). Furthermore, we have used these temporal bias-corrected DEMs as input in GlabTop
199 and GlabTop2 models to estimate glacier volumes rather than change in surface volume (or
200 DEM differencing). The models have their own uncertainties, as discussed in the later section,
201 which are well-above any jitter-induced errors and did not make any notable difference in the
202 GlabTop model results.

203 The bias corrected DEMs were further used to estimate the volume of glaciers of the study
204 area. We estimated the volume using three different methods, i.e., Glacier Bed Topography
205 model (GlabTop2), shear-stress/slope dependent (hereafter slope dependent method) and area-

206 related methods. GlabTop2 model is the upgraded version of the previous GlabTop model
 207 developed by (Linsbauer et al., 2009) where the thickness is estimated at several points along
 208 the glacier branch lines further interpolating to the entire glacier (Linsbauer et al., 2009; Paul
 209 and Linsbauer et al., 2012; Frey et al., 2014). In the advanced GlabTop2 model, the thickness
 210 is calculated for randomly selected DEMs pixel within the glacier inner cells (or glacierised
 211 area). Thickness of all other glacier cells are estimated by interpolating the thickness at random
 212 cells and the ice thickness at the glacier marginal cells (or along glacier margins) where ice
 213 thickness is known to be zero (Frey et al., 2014; Ramsankaran et al., 2018). The calculation is
 214 distributive, requires only DEM and glacier outline as input and uses Equation 1 (Cuffey and
 215 Paterson, 2010; Haeberli and Hoelzle, 1995).

$$216 \quad hf = \frac{\tau}{f \rho g \sin(\alpha)} \quad (1)$$

217 where

218 τ = average basal shear stress along the central flow line

219 f = shape factor (60-90; Cuffey and Paterson, 2010)

220 ρ = density of ice (900 kg m⁻³)

221 g = acceleration due to gravity (9.8 m s⁻²)

222 α = mean surface slope

223

224 The value of basal shear stress (in kPa) is estimated using an empirical relationship between
 225 basal shear stress and glacier elevation range (ΔH , in km) as per Equation 2 (Haeberli and
 226 Hoelzle, 1995)

$$227 \quad \tau = \left(\begin{array}{l} 0.5 + 159.8 \Delta H - 43.5 (\Delta H)^2 \\ 150 \end{array} \quad \begin{array}{l} \Delta H \leq 1.6 \text{ km} \\ \Delta H > 1.6 \text{ km} \end{array} \right) \quad (2)$$

228

229 Slope dependent method uses the same equation (1 and 2), as Glabtop and Glabtop2 model, to
230 calculate the average thickness of a glacier. To account the semi-elliptical cross-sectional
231 geometry of a glacier, a multiplication with 0.785 is added to equation 1. This method has been
232 applied extensively by many (Hoelzle et al., 2007; Paul and Svoboda, 2009; Salzmann et al.,
233 2013). However, area-related thickness estimation only uses surface area of the glacier and
234 other scaling parameters. It is the most frequently used method because of its simple and fast
235 implementation. Equation 3, given below, is used for area-related thickness estimation.

$$236 \quad H = cA^\gamma \quad (3)$$

237 Where

238 H = mean thickness of glacier

239 c and γ = scaling parameters given by Chen and Ohmura (1990) who used 63 glaciers and Bahr
240 et al. (1997) who used theoretical analysis to determine these parameters.

241

242 The obtained thickness from slope-dependent and area-scaling method was then used to
243 calculate the volume of glaciers with the help of glacierised areas of the respective years. The
244 pixel-based thickness obtained from the GlabTop2 model was first applied to calculate the
245 volume of each pixel and further summing up all the pixel to get the volume of individual
246 glacier volume.

247

248 ***3.3. build-up, vegetation, and water body mapping***

249 Both Corona and PlanetScope images were used to map the built-up, vegetation and water
250 bodies of 1969 and 2018, respectively. Owing to lesser heterogeneity of the landscape, a
251 supervised classification technique on 1969 and 2018 images was used to distinguish between
252 vegetation and non-vegetation land in ArcGIS 10.4, with additional manual correction where

253 needed. The classification process included 15 training samples containing >30,000 pixels
254 combined to improve the classifier's overall performance. Built-up area of 2018 were manually
255 digitised on screen using high resolution PlanetScope image. The 2018 results were overlaid
256 on the 1969 corona image as a reference to digitise the built-up area of 1969. The built-up areas
257 of 2018 which were not present or cannot be identified on 1969 images were removed from
258 1969 built-up areas. The built-up areas which no longer exist at present but were present in
259 1969 also mapped and added. Water-bodies were mapped manually on screen on both Corona
260 and PlanetScope images.

261 *3.4. Climate data analysis*

262 In addition to the satellite imageries, long-term ERA5 monthly single level reanalysis climate
263 data have also been used in the study to understand the climatic settings of the study area.
264 ERA5 (downloaded from <https://climate.copernicus.eu/>) is a 5th generation European Centre
265 for Medium-Range Weather Forecasts (ECMWF) reanalysis high resolution climate data at
266 0.25 degrees. The data carries a large set of variables from 1979 to present. In this study,
267 monthly mean temperature and precipitation data was used. In-situ data from Leh, India
268 (nearest in-situ data available) was used to bias correct the ERA5 temperature and precipitation.
269 Kanda et al., 2020 evaluated the performance of seven grid-based datasets against the observed
270 data from 19 in-situ stations across the region of Karakoram, Greater and Lower western
271 Himalaya and found that ERA-Interim (precipitation), and CRU-TS and ERA-Interim
272 (temperature) are the best performing datasets in all these regions with additional bias
273 corrections. ERA5 is the improved version of ERA-Interim and can be used for further analysis
274 (Figure 4).

275 Linear scaling bias correction (Ines and Hansen 2006; Teutschbein and Seibert 2012, Shrestha
276 et al 2016) was adopted for ERA5 data correction with the help of Leh in-situ data. The bias

277 corrected Leh data was statistically analysed to understand the magnitude and significance of
278 trends using Mann-Kendall test and Sen's slope estimator (Sen, 1968), respectively. The
279 change in temperature and precipitation (Table 2) was calculated using Equation 4 following
280 Shukla et al 2020:

$$281 \text{ Change} = (\beta \times L)/M \quad (4)$$

282 Where β is Sen's slope estimator, L is the length of the period and M is the long-term mean.

283

284 ***3.5. Uncertainty assessment***

285 Our study involves extraction of various key environmental parameters utilizing multiple
286 satellite data and methods. Hence, there are different sources of uncertainties related to the
287 approaches used in the present study. Therefore, in this section we present the methodologies
288 that were used to estimate the uncertainties.

289 ***3.5.1. Uncertainties in glacierised area and volume:***

290 Since there is no available in-situ reference data for large set of glaciers in this region.
291 Therefore, we estimate the error term based on a buffer based assessment for each glacier
292 following the methods of Bolch et al., 2010; Granshaw & G. Fountain, 2006; Mölg et al., 2018;
293 Tielidze & Wheate, 2018. The buffer width was set to half-pixel as the glaciers of the study
294 area are debris free. The half-pixel buffer was applied to the glacier polygons and area was
295 recalculated. The overall uncertainty was $\sim \pm 3.4\%$ with individual uncertainties of $\pm 0.6, 3.9,$
296 $4.0, 4.1$ and 4.2% for 1969, 1991, 1998, 2010 and 2019 images (Table 3).

297 For GlabTop2 and Slope dependent method the uncertainties were estimated based on error
298 propagation method (Kumari et al., 2021; Ramsankaran et al 2018; Frey et al., 2014) by
299 modifying the scaling parameters. Since the variation in these parameters are unknown for the

300 study area, $\pm 5\%$ of uncertainty was considered for τ , f (Driedger and Kennard 1986; Haeberli
301 and Hoelze, 1995; Kumari et al 2021; Ramsankaran et al 2018) and $\pm 10\%$ was considered for
302 the density of ice (ρ) following Gantayat et al. (2014). The uncertainty in the term $u(\sin \alpha)/\sin$
303 α was assumed to be ± 0.2 considering the potential uncertainty of $\sim 20\text{m}$ in ASTER DEM in
304 the Himalayan region (Bhambri et al., 2011; Toutin 2008). The uncertainty in the area-related
305 volume estimation was determined by comparing the influence of the two applied scaling
306 parameter sets on the results with additional modification of $\pm 5\%$ in individual glacier area
307 (Frey et al., 2014). Table 4 present the associated uncertainties.

308

309 *3.5.2. Uncertainties in other environmental parameters:*

310 The uncertainty in the build-up and lake area was estimated based on a comparison between
311 the independently generated outlines in two sample villages (Chuchot and Stok) and all the
312 lakes by three different analyst on the same satellite images. For vegetation cover, a stratified
313 random sampling design was used to determine the sample numbers and their position on the
314 map. For the purpose we have selected ~ 500 points on both Corona and PlanetScope images.
315 The accuracy assessment was done by determining the probability of a particular cell value
316 being similar to the actual generated classified information (i.e. vegetation cover). Error matrix
317 (also known as confusion matrix or covariance matrix) and kappa coefficient was calculated
318 for both Corona and PlanetScope. Details of the uncertainties are presented in Table 5.

319 **4. Results and discussion**

320 *4.1. Overall change in key environmental parameters between 1969 and 2021*

321 We analysed several key environmental parameters in the study area, i.e., glacierised area and
322 volume, built-up area, vegetation area, lake area, and demography between 1969 and 2021.
323 Due to limitations in temporal datasets, the time periods for the analyses are different. The

324 glacierised region was mapped for 1969, 1991, 1998, 2010 and 2019. Glacier volume was
325 estimated for 2004 and 2020 due to non-availability of cloud-free DEMs before 2004. Built-
326 up, vegetation and lake areas were analysed for two periods (1969 and 2018) because publicly
327 no high-resolution images exists in between. The population data is also not available after
328 census 2011, therefore population of 2021 was extrapolated through a regression developed
329 using available datasets of from 1971, 1981, 2001 and 2011 census reports.

330 *4.1.1. Overall change in glacierised area and volume*

331 Stok and Kang Yatze watersheds consist of 30 and 106 glaciers, larger than 0.01 km², covering
332 an area of 10.6 and 78.5 km², respectively. These glaciers retreated over time with varying
333 retreat rates during different periods. Glaciers of Stok region retreated at a rate of 0.26, 0.35,
334 0.6, and 0.57% per year during the periods 1969-91, 1991-98, 1998-2010, and 2010-19,
335 respectively. Total change observed over 50 years was 2.51 km², equivalent to 19%
336 (0.38%/year) of the total glacierised area. Whereas, Kang Yatze region observed a slightly
337 different rate of change during individual periods. However, total change (in %) in glacierised
338 area over 50-year period was similar to Stok region, i.e., 18.7 km², equivalent to 19%
339 (0.38%/year). The retreat rate in Kang Yatze was found to be 0.38, 0.28, 0.62, and 0.33% per
340 year for 1961-91, 1991-98, 1998-2010, and 2010-19, respectively. Overall, glacierised area
341 changed from 110.4 km² in 1969 to 89.21 km² in 2019 with a change of 21.2 km², equivalent
342 to 19% (0.38%/year) of the glacierised area over 50-year period. These changes are however
343 higher than the changes observed by Negi et al., 2021 and Shukla et al, 2020 in the adjacent
344 region of Shayok (Karakoram region) and Suru (Kargil region) where the retreat was reported
345 to be 7.8% (0.008%/year) and 6% (0.2%/year), respectively. Negi et al., 2021 studied 569
346 glaciers of size greater than 1 km² of Shayok region between 1991 and 1994. Whereas, Shukla
347 et al., 2020 studied glaciers larger than 0.01 km² between 1971 and 2017. However, Schmidt
348 and Nüsser, 2017 studied glaciers (> 0.03 km²) of Stok, Kang Yatze and the region nearby

349 between 1969-2016 and found results similar to the present study. These results are interesting
350 considering that our study area is the most populous and tourism-prone within Ladakh region,
351 and the significantly higher glacier retreats clearly point towards a plausible connection
352 between glaciers and threatened microclimate. Figure 2, 3, 5 and 8 presents the area changes
353 over 50-year period while Figure 4 provides the data on climate changes in this region.

354 Two (GlabTop2 model and area-scaling method) of the three methods used in this study to
355 estimate the thickness of these ice masses gave similar results; however, the third method
356 (slope-dependent method) gave comparatively lower thickness estimate. Volume of glaciers in
357 Stok region using GlabTop2, area-scaling and slope-dependent method was found to be 0.29,
358 0.31 and 0.22 km³, respectively, for the year 2004; and 0.23, 0.27 and 0.17 km³ for the year
359 2020, respectively. Volume of glaciers in Kang Yatze region using GlabTop2, area-scaling and
360 slope-dependent method was found to be 3.2, 3.1, and 2.1 km³, respectively, for the year 2004
361 and 2.6, 2.8, and 1.7 km³ for the year 2020, respectively. Figure 2, 3, 5 and 8 present the average
362 values of these estimates over 16-year period. The average (of the three different estimates)
363 change found over the 16-year period was 0.05 and 0.37 km³, equivalent to 18% and 13% (1.1
364 and 0.8%/year) in the total ice reserve of Stok and Kang Yatze region, respectively. The study
365 area currently holds ~2.5 Gigaton (Gt) of water with 0.21 and 2.5 Gt of water in the glaciers of
366 Stok and Kang Yatze regions, respectively.

367 Changes in the glaciers of high-altitude Himalayan region are generally due to the rise in
368 temperature, orientation, debris and black carbon among others. However, in the region around
369 Leh, these changes are also associated with the lower winter precipitation (Soheb et al., 2020).
370 Region around Leh (study area) generally receives comparatively less precipitation (Figure 4)
371 (Soheb et al., 2020; Schmidt and Nüsser 2017), and together with the rise in temperature the
372 impact will be comparatively higher on these glaciers. It is evident that the glacierised region
373 around Leh is losing mass at a higher pace despite being in a higher altitude region between

374 Karakoram and other western Himalayan region. The higher retreat can be due to the presence
375 of smaller glaciers in high numbers in Ladakh (Schmidt and Nüsser, 2017). These glaciers are
376 more prone to rise in temperature and decline in solid precipitation due to their short response
377 time, and they are most probably vulnerable to local climatic variations. Leh showed an
378 increment of 0.04, 0.05 and 0.03 °C/year in annual, JJAS and winter temperature, respectively,
379 at $p < 0.05$ (95% percent confidence level) through Man-Kendal test and Sen's slope estimator
380 (Sen, 1968). However, the trend estimated in precipitation is negative but not statistically
381 significant to conclude any inferences from it (Table 2).

382 The decline of glaciers in such environment is of serious concern as it directly impacts
383 livelihood, ecosystem and socio-economic dimensions of the region because of their higher
384 dependency on glacier meltwater streams. The residents of the region have witnessed a decline
385 in agricultural yields, the main driver of economic development of the region, due to a decrease
386 in water resources (Barrett and Bosak 2018). The water scarcity together with the recent boom
387 in tourism activity (tourism footprint in Leh was 327,366 in 2018, a number that is more than
388 the entire population of Ladakh) has led to a shift in livelihood from agriculture to other
389 commercial activities (Müller et al. 2020), though even the latter relies heavily on water
390 resources. To cope with water scarcity, some people of Ladakh have developed new water
391 management techniques, commonly known as 'ice reservoirs' or 'ice stupas', to supplement
392 agricultural activities (Nüsser, et al., 2019a,b).

393

394 *4.1.2. Overall changes in Vegetation, built-up areas and lakes*

395 Vegetation cover of within the village vicinity of a catchment was analysed in this study. Two
396 entire glacier catchments of Kang Yatze region were also excluded from this analysis because
397 no settlement exist in those remote catchments. Vegetation cover of overall study area is

398 presented in Figure 5, 6, 7 and 8 along with the % change in 49 years. Four villages namely
399 Chuchot, Stakna, Changa and Hemis are also included in the Stok region because they are
400 partially fed by the meltwater coming from the Stok range. However, Hemis village is the only
401 village in this study which is not fed by any glacier. The source of water for Hemis village is
402 snowmelt and most probably springs within the catchment as the catchment does not have any
403 glacier but comprise one of the oldest Monastery (Hemis monastery), village and vegetation.

404 Stok region consists of several villages in which Rumbak, Stok, Matoo, Martselang and Shang
405 are completely fed by the glaciers of this region. Whereas, all the villages in Kang Yatze region
406 i.e., Upshi, Miru, Lato, Gya, Sa-Soma and Runtse are entirely fed by the glaciers of Kang
407 Yatze region. In 1969, the vegetation area was found to be 17.2 and 2.8 km² in Stok and Kang
408 Yatze region, respectively. Whereas, vegetation cover decreased over time in Stok region as a
409 whole to 14 km² and increased in Kang Yatze region to 3.15 km². However, in few villages of
410 Stok and Kang Yatze region, vegetation increased significantly. These significant changes are
411 discussed in the village-level section (Section 4.2). The change observed over 49 years period
412 was found to be -3.2 and 0.34 km² equivalent to -18.4 (-0.38 %/year) and 12.1 % (0.25 %/year)
413 in Stok and Kang Yatze regions, respectively.

414 Overall, the vegetation cover decreased in the study area from 20.1 km² in 1969 to 17.2 km² in
415 2018. The total change found was -2.8 km² equivalent to -14.1 % (-0.29 %/year) in the entire
416 study area in 49-year period (1969-2018). It should be noted that both the images (Corona and
417 PlanetScope) used in this study are from summer pre-harvesting period to achieve minimum
418 uncertainty. It is also possible that during these particular years (1969 or 2018) the harvest was
419 good due to plenty of water or farming was abandoned due to lack of water, disaster or societal
420 disputes thus raising the level of uncertainty in estimating the actual scenario. We made every
421 possible effort to avoid such issues, and consulted Google Earth temporal image collections
422 and other cloud free PlanetScope imageries of immediate years.

423 Built-up sites of the Stok and Kang Yatze regions increased from 0.61 and 0.15 km² in 1969 to
424 2.27 and 0.3 km² in 2018, with a change in 1.66 and 0.15 km² equivalent to 272 % (5.6 %/year)
425 and 100% (2.1 %/year), respectively. Increase in built-up areas are directly associated with the
426 increase in connectivity of the region. The road network in this region increased significantly
427 with an increase from 81 and 61 km in 1969 to 250 and 105 km in 2018 in Stok and Kang
428 Yatze region, respectively. The rise in road network was found to be 169 km (209 % at 4.3
429 %/year) and 44 km (72 % at 1.5 %/year) in Stok and Kang Yatze region, respectively. A
430 comparatively less change in road network in Kang Yatze region was because all of these
431 villages lie directly on the Leh-Manali highway and majority of the road remained same over
432 these years except some link roads within these narrow villages.

433 The villages of Stok region are mostly away from major highways and thus multiple roads
434 linking these villages were made. The mining activity (of gravel for constructions) within the
435 study area are entirely situated in Stok region's alluvial fan, thus giving rise to Built-up area
436 and road network. Villages which were inaccessible for vehicular activity in 1969 are now
437 accessible in 2018. Overall, an increase of 1.81 km² (238 % at 4.9 %/year) and 213 km (150 %
438 at 3.1 %/year) of built-up area and road network was observed in the entire study area,
439 respectively. Figure 5, 6, 7 and 8 presents the built-up area and % change over 49-year period
440 between 1969 and 2018. Local population in the study area has grown more than double its
441 size in 50 years at a rate of 2.3 %/year. This has led to an increase in built-up activities in the
442 region. Also, the booming tourism industry with a 600+ fold in tourism footprint (Dame et al.,
443 2019; Müller et al., 2020) over the years has initiated over exploitation of natural resources and
444 unplanned urbanisation. The easy money in this industry has caused a shift in local economy
445 from agriculture to tourism thus rendering the once cultivable land more prone to degradation
446 and desertification.

447 Number of lakes increased from 15 lakes (2 in Stok and 13 in Kang Yatze region) in 1969 to
448 36 lakes (5 in Stok and 31 in Kang Yatze region) in 2018. Total lake area of Stok and Kang
449 Yatze regions changed from 0.009 and 0.24 km² in 1969 to 0.02 and 0.52 km² in 2018,
450 respectively. Figure 1, 2, 3 and 5 presents the lake location, area and % change in area in 49
451 years. Overall, change in lake area of the study area was found to be 0.3 km² equivalent to 122
452 % at a rate of 2.5 %/year. Identification of higher altitude lakes formed due to glacial retreat or
453 moraine dammed lake are extremely important in this age when glacial lake outburst floods
454 (GLOFs) are on the rise. GLOFs alone can be devastating especially when unplanned
455 urbanisation in the downstream valleys is happening. Flash flood of Kedernath in 2013 and
456 GLOF of Gya valley (Kang Yatze region) in 2014 (Schmidt et al., 2020; Majeed et al., 2021)
457 are some of the few examples of such events.

458

459 ***4.2. Village level change in key environmental parameters***

460 Regional level change of key environmental parameters, already discussed in previous sections,
461 was not sufficient to explain the changes in detail. Therefore, we have also analysed the
462 changes at village-scale. Tuchik, a catchment between Matoo and Martselang catchment,
463 constitute insignificant amount of vegetation cover and no population or settlement area.
464 Though, it is not a village but understanding this catchment is important from a glaciological
465 perspective. This catchment holds only one glacier of Stok region with an area of 0.12 km²
466 (2019) and lost half of its area (0.12 km², 1 %/year) in last 50 years (1969-2019).

467 Martselang on the other hand also showed similar but comparatively lower change in total area
468 loss of 38% (0.68 km², 0.8 %/year) followed by Upshi, Matoo and Rumbak catchment with 19
469 (8.04 km², 0.38 %/year), 18.9 (0.93 km², 0.38 %/year) and 17% (0.38 km², 0.34 %/year) loss
470 in total glacierised area in 50-year period, respectively. The common element between glaciers

471 of Tuchik and Martselang catchment is the glacier size i.e., very small ($\sim 0.2 \text{ km}^2$), therefore
472 the results indicate that glaciers of smaller sizes are more prone to retreat as compared to
473 glaciers with a higher surface area. A small change in equilibrium line altitude or snow line
474 altitude can expose these small glaciers entirely to melting thus losing a relatively higher
475 surface area over time. Whereas glaciers of Stok and Sku-Markha catchment lost comparatively
476 least relative glacierised area of 11.7 % (0.46 km^2 , 0.23 %/year) and 11.4 % (3.48 km^2 , 0.23
477 %/year), respectively. Since, the volume of glacier is related to the glacier area, therefore
478 change in glacier volume is expected to follow the similar trend over 50-year period. The total
479 volume change was found to be -38%, -15%, -15%, -21%, -25%, -15% and -12% in Tuchik,
480 Rumbak, Stok, Matoo, Martselang, Upshi and Sku-Markha village catchments, respectively.

481 Built-up change was found to be inversely proportional to the vegetation of the village. Highest
482 increase in built-up area was found in Stok village (688%) followed by Changa (247%),
483 Chuchot (246%), Matoo (225%) and Hemis (205%). The nearly seven-fold rise in built-up area
484 of Stok village is because of the seven-mining activity within the vicinity of village area. Road
485 network in the vicinity of Stok village also increased significantly (380%) and is the highest
486 among all the villages of the study area. Road network of Martselang also increased
487 significantly (368%) followed by Matoo (253%), Changa (141%) and Chuchot (111%).
488 Whereas, comparatively lowest increase in built-up area was found in Sku-Markha, Upshi, and
489 Stakna with 62%, 122% and 134 % increase over 50-year period, respectively. Road network
490 in some of these villages are also lowest among the study area with 8% and 28% in Upshi and
491 Stakna. One of the main reasons for such low built-up area and road network is because of the
492 two agricultural farms (one in each Stakna and Upshi) established in recent times (2005), a
493 result of Igu-Phey canal which turned these barren lands into an irrigated farm (GJK, 2011;
494 Nüsser et al 2012).

495 Vegetation of Upshi (48%), Changa (87%) and Rumbak (29.4%) increased whereas a decrease
496 in vegetation was observed in other villages over 40-year period. Increase in vegetation of
497 Upshi and Changa is the outcome of Igu-Phey canal which gave these barren lands an extra
498 source of water for irrigation. Our results are in agreement with GJK, 2011 and Nüsser et al
499 2012. The barren land around Stakna has also been turned into a full-fledged agricultural and
500 animal farm and expected to grow in coming years. Construction of such canals needs to be
501 undertaken to supply water to those regions which has the potential for agricultural activity to
502 increase food production of the region. Increase in built-up area and road network and decrease
503 in vegetation is directly linked to the increase in population. Highest population growth was
504 seen in Chuchot, Changa, Stok and Matoo with an increase of 158%, 132%, 112% and 72% in
505 last 50 years (1971-2021). Whereas lowest growth in population was observed in Hemis,
506 Rumbak and Sku-Markha with 33%, 38% and 53%, respectively. Figure 8 presents the change
507 in all the key environmental parameters at a village level between 1969 and 2021.

508

509 **5. Conclusion**

510 In this study we analysed key environmental parameters including area and volume of 136
511 glaciers, built-up and vegetation of 13 villages, area of 36 lakes and demography of 13 major
512 villages around Leh between 1969 and 2021. The area change of glaciers was obtained using
513 freely available Corona and Landsat imageries with additional aid from PlanetScope image and
514 Google Earth. A comparatively higher retreat (~ 19 at 0.38 %/year) in the glacierised area was
515 found in 50 years as compared to the adjacent region of Shayok and Suru. The retreat was even
516 higher (~ 35 -50%) in very small glaciers of area ~ 0.02 km². Volume of glaciers also decreased
517 over time with a reduction of 0.42 km³ equivalent to ~ 13 % (0.8 %/year) of the volume in 16-
518 year period. At present, the study area holds 2.5 Gt of water in these glaciers.

519 A decrease (-5 to -58%) in vegetation was found in majority of the villages except Rumbak
520 (29%), Upshi (48%) and Changa (87%) where vegetation significantly increased over 49-year
521 period. The 43 km long Igu-Phey canal played a major role in such increase in vegetation.
522 Increase in built-up area (688%) and road network (380%) was found highest in Stok village
523 due to seven gravel mining activity in the area whereas, other village witnessed comparatively
524 lower increase in built-up area (63-275%) and road network (8-368%). An inverse relationship
525 was found between % change of vegetation and % change of Built-up area. Increase in
526 population growth percentage was also found highest in Stok (112%), Changa (132%) and
527 Chuchot (157%) whereas in other villages the population growth was comparatively lower (32-
528 72%). One of the major reasons for higher increase in built-up areas and road network, and a
529 decrease in vegetation is most probably the tourism industry as tourist footprint in last 44 years
530 was 620 times (527 in 1974 to 327366 tourists in 2018). Another factor for such change can
531 also be attributed to government and defence related activities which is expected to grow in
532 coming years due to redesignation of Ladakh as a Union Territory. Formation of new lakes
533 were also observed in 49 years. Number of lakes increased from 15 to 36 with an increase in
534 area from 0.25 km² to 0.55 km² equivalent to 122% change in lake area between 1969 and
535 2018.

536 While research and policy focus is slowly falling on Leh City and its vicinity, our study proves
537 that environmental changes are happening at a higher rate in rural regions around Leh. A proper
538 assessment and a detailed future planning are very much required in rural regions as well.
539 Systematically documenting these changes using multisource datasets for a larger region can
540 provide more holistic picture of the effects which these mountains are experiencing under the
541 contemporary climate change and demographic shifts.

542

543 **6. Acknowledgement**

544 The authors would like to thank USGS for Corona and Landsat imageries, Planet.com for
545 PlanetScope imagery, NASA for ASTER DEM and The European Centre for Medium-Range
546 Weather Forecasts (ECMWF) for ERA5 reanalysis temperature and precipitation data. We are
547 grateful to Ms. Prerna Joshi for the insights and help in this study. The authors are also thankful
548 to the editor, scientific editor and the two anonymous reviewers for their critical review of the
549 manuscript.

550 **7. Data availability statement**

551 The data that support the findings of this study are available on request from the lead author.
552 The data belongs to the lead author's PhD program and cannot be made public for now.

553 **8. References**

554 Andreassen, L. M., Paul, F., Kaab, A., & Hausberg, J. E. (2008). Landsat-derived glacier
555 inventory for Jotunheimen, Norway, and deduced glacier changes since the 1930s. *The*
556 *Cryosphere*, 16.

557 Arrowsmith, C., & Inbakaran, R. (2002). Estimating environmental resiliency for the
558 Grampians National Park, Victoria, Australia: a quantitative approach. *Tourism Management*,
559 23(3), 295-309.

560 Barrett, K., & Bosak, K. (2018). The Role of Place in Adapting to Climate Change: A Case
561 Study from Ladakh, Western Himalayas. *Sustainability*, 10(4), 898.
562 <https://doi.org/10.3390/su10040898>

563 Bahr, D. B., Meier, M. F., & Peckham, S. D. (1997). The physical basis of glacier volume-area
564 scaling. *Journal of Geophysical Research: Solid Earth*, 102(B9), 20355–20362.
565 <https://doi.org/10.1029/97JB01696>

- 566 Bhambri, R., Bolch, T., Kawishwar, P., Dobhal, D. P., Srivastava, D., & Pratap, B. (2013).
567 Heterogeneity in glacier response in the upper Shyok valley, northeast Karakoram. *The*
568 *Cryosphere*, 14.
- 569 Bhambri, Rakesh, Bolch, T., Chaujar, R. K., & Kulshreshtha, S. C. (2011). Glacier changes in
570 the Garhwal Himalaya, India, from 1968 to 2006 based on remote sensing. *Journal of*
571 *Glaciology*, 57(203), 543–556. <https://doi.org/10.3189/002214311796905604>
- 572 Bhardwaj, A., Joshi, P. K., Sam, L., Singh, M. K., Singh, S., & Kumar, R. (2015). Applicability
573 of Landsat 8 data for characterizing glacier facies and supraglacial debris. *International Journal*
574 *of Applied Earth Observation and Geoinformation*, 38, 51-64.
- 575 Bhardwaj, A., Joshi, P. K., Singh, M. K., Sam, L., & Gupta, R. D. (2014). Mapping debris-
576 covered glaciers and identifying factors affecting the accuracy. *Cold Regions Science and*
577 *Technology*, 106, 161-174.
- 578 Bhardwaj, A., Kumar, R., & Sam, L. (2019). Analysing Geospatial Techniques for Land
579 Degradation Studies in Hindu Kush-Himalaya. In *Environmental Change in the Himalayan*
580 *Region* (pp. 117-135). Springer, Cham.
- 581 Bolch, T., Menounos, B., & Wheate, R. (2010). Landsat-based inventory of glaciers in western
582 Canada, 1985–2005. *Remote Sensing of Environment*, 11.
- 583 Bray, J. (1991). Ladakhi history and Indian nationhood. *South Asia Research*, 11(2), 115-133.
- 584 Buckley, R. C., Pickering, C. M., & Warnken, J. (2000). Environmental Management for
585 Alpine Tourism and Resorts in. *Tourism and development in mountain regions*, 27-45.
- 586 Buntaine, M. T., Mullen, R. B., & Lassoie, J. P. (2007). Human use and conservation planning
587 in Alpine areas of Northwestern Yunnan, China. *Environment, Development and*
588 *Sustainability*, 9(3), 305-324.

- 589 Census of India (2011) Census of India 2011. Retrieved January 12, 2021 from -
590 <https://www.census2011.co.in/census/district/621-leh.html>
- 591 Chen, J. and Ohmura, A.: Estimation of Alpine glacier water resources and their change since
592 the 1870s, IAHS Publications – Hydrology in Mountainous Regions, I – Hydrological
593 Measurements; the water cycle, Proceedings of two Lausanne Symposia, August 1990, edited
594 by: Lang, H. and Musy, A., IAHS Publ., 193, 127–135, 1990.
- 595 Cuffey, K., & Paterson, W. S. B. (2010). *The physics of glaciers* (4th ed). Butterworth-
596 Heinemann/Elsevier.
- 597 Dame, J., Schmidt, S., Müller, J., & Nüsser, M. (2019). Urbanisation and socio-ecological
598 challenges in high mountain towns: insights from Leh (Ladakh), India. *Landscape and urban*
599 *planning*, 189, 189-199.
- 600 Draper, D. (2000). Toward sustainable mountain communities: Balancing tourism
601 development and environmental protection in Banff and Banff National Park, Canada.
602 *AMBIO: A Journal of the Human Environment*, 29(7), 408-415.
- 603 Frey, H., Machguth, H., Huss, M., Huggel, C., Bajracharya, S., Bolch, T., Kulkarni, A.,
604 Linsbauer, A., Salzmann, N., & Stoffel, M. (2014). Estimating the volume of glaciers in the
605 Himalayan–Karakoram region using different methods. *The Cryosphere*, 8(6),
606 2313–2333. <https://doi.org/10.5194/tc-8-2313-2014>
- 607 GJK (Government of Jammu and Kashmir) 2011. *Evaluation Report On Igophey Canal, Leh*
608 *Ladakh (Joint Vernture of Irrigation Division Igophey and CAD Leh) (1979 – 2011)*.
609 Directorate of Economics and Statistics, J&K Planning and Development Department.

- 610 Garg, P. K., Shukla, A., & Jasrotia, A. S. (2019). On the strongly imbalanced state of glaciers
611 in the Sikkim, eastern Himalaya, India. *Science of The Total Environment*, 691, 16–35.
612 <https://doi.org/10.1016/j.scitotenv.2019.07.086>
- 613 Geneletti, D., & Dawa, D. (2009). Environmental impact assessment of mountain tourism in
614 developing regions: A study in Ladakh, Indian Himalaya. *Environmental impact assessment*
615 *review*, 29(4), 229-242.
- 616 Haeberli W, Hölzle M (1995) Application of inventory data for estimating characteristics of
617 and regional climate-change effects on mountain glaciers: a pilot study with the European Alps.
618 *Annals of Glaciology* 21: 206-212.
- 619 Hoelzle, M., Chinn, T., Stumm, D., Paul, F., Zemp, M., & Haeberli, W. (2007). The application
620 of glacier inventory data for estimating past climate change effects on mountain glaciers: A
621 comparison between the European Alps and the Southern Alps of New Zealand. *Global and*
622 *Planetary Change*, 56(1–2), 69–82. <https://doi.org/10.1016/j.gloplacha.2006.07.001>
- 623 Ines, A. V. M., & Hansen, J. W. (2006). Bias correction of daily GCM rainfall for crop
624 simulation studies. *Agricultural and Forest Meteorology*, 10.
- 625 Kanda, N., Negi, H. S., Rishi, M. S., & Kumar, A. (2020). Performance of various gridded
626 temperature and precipitation datasets over Northwest Himalayan Region. *Environmental*
627 *Research Communications*, 2(8), 085002. <https://doi.org/10.1088/2515-7620/ab9991>
- 628 Khan, A., Naz, B. S. & Bowling, L. C. Separating snow, clean and debris covered ice in the Upper
629 Indus Basin, Hindukush-Karakoram-Himalayas, using Landsat images between 1998 and 2002. *Journal*
630 *of Hydrology* **521**, 46-64 (2015).
- 631 Linsbauer, A., Paul, F., & Haeberli, W. (2012). Modeling glacier thickness distribution and
632 bed topography over entire mountain ranges with GlabTop: Application of a fast and robust

- 633 approach: REGIONAL-SCALE MODELING OF GLACIER BEDS. *Journal of Geophysical*
634 *Research: Earth Surface*, 117(F3), n/a-n/a. <https://doi.org/10.1029/2011JF002313>
- 635 Linsbauer, A., Paul, F., Hoelzle, M., Frey, H., & Haerberli, W. (2009). *The Swiss Alps Without*
636 *Glaciers – A GIS-based Modelling Approach for Reconstruction of Glacier Beds*. 6.
- 637 Majeed, U., Rashid, I., Sattar, A., Allen, S., Stoffel, M., Nüsser, M., Schmidt S. (2021)
638 Recession of Gya Glacier and the 2014 glacial lake outburst flood in the Trans-Himalayan
639 region of Ladakh, India. *Science of the Total Environment*, 756:144008. doi:
640 10.1016/j.scitotenv.2020.144008
- 641 Messerli, B., & Ives, J. D. (1997). *Mountains of the world: a global priority*. Parthenon, New
642 York.
- 643 Michaud, J. (1991). A social anthropology of tourism in Ladakh, India. *Annals of Tourism*
644 *Research*, 18(4), 605-621.
- 645 Moss, L. A., & Godde, P. M. (2000). Strategy for future mountain tourism. *Tourism and*
646 *development in mountain regions.*, 323-338.
- 647 Müller, J.; Dame, J.; Nüsser, M. Urban Mountain Waterscapes: The Transformation of Hydro-
648 Social Relations in the Trans-Himalayan Town Leh, Ladakh, India. *Water* **2020**, 12, 1698.
649 <https://doi.org/10.3390/w12061698>
- 650 Muhammad, S., Gul, C., Muneer, J. & Waqar, M. M. Efficiency of classification techniques
651 for sachen and rupal glaciers variation during 1972–2010. *International Conference on*
652 *Aerospace Science & Engineering (ICASE), IEEE International*, 1-3 (2013).
- 653 Muhammad, S., Tian, L., & Khan, A. (2019). Early twenty-first-century glacier mass losses in
654 the Indus Basin constrained by density assumptions. *Journal of Hydrology*, 574, 467-475.

- 655 Nagai, H., Fujita, K., Sakai, A., Nuimura, T. & Tadono, T. Comparison of multiple glacier
656 inventories with a new inventory derived from high-resolution ALOS imagery in the Bhutan
657 Himalaya. *The Cryosphere* 10, 65-85, doi:10.5194/tc-10-65-2016 (2016).
- 658 Negi, H. S., Kumar, A., Kanda, N., Thakur, N. K., & Singh, K. K. (2021). Status of glaciers
659 and climate change of East Karakoram in early twenty-first century. *Science of The Total*
660 *Environment*, 753, 141914. <https://doi.org/10.1016/j.scitotenv.2020.141914>
- 661 Nepal, S. K., & Chipeniuk, R. (2005). Mountain tourism: Toward a conceptual framework.
662 *Tourism Geographies*, 7(3), 313-333.
- 663 Nüsser, M., Dame, J., Kraus, B., Baghel, R., & Schmidt, S. (2019). Socio-hydrology of
664 “artificial glaciers” in Ladakh, India: Assessing adaptive strategies in a changing cryosphere.
665 *Regional Environmental Change*, 19(5), 1327–1337. [https://doi.org/10.1007/s10113-018-](https://doi.org/10.1007/s10113-018-1372-0)
666 [1372-0](https://doi.org/10.1007/s10113-018-1372-0)
- 667 Nüsser, M., Schmidt, S., & Dame, J. (2012). Irrigation and Development in the Upper Indus
668 Basin: Characteristics and Recent Changes of a Socio-hydrological System in Central Ladakh,
669 India. *Mountain Research and Development*, 32(1), 51–61. [https://doi.org/10.1659/MRD-](https://doi.org/10.1659/MRD-JOURNAL-D-11-00091.1)
670 [JOURNAL-D-11-00091.1](https://doi.org/10.1659/MRD-JOURNAL-D-11-00091.1)
- 671 Nuth, C., & Kääb, A. (2011). Co-registration and bias corrections of satellite elevation data
672 sets for quantifying glacier thickness change. *The Cryosphere*, 5(1), 271–290.
673 <https://doi.org/10.5194/tc-5-271-2011>
- 674 Paul, F., & Kääb, A. (2005). Perspectives on the production of a glacier inventory from
675 multispectral satellite data in Arctic Canada: Cumberland Peninsula, Baffin Island. *Annals of*
676 *Glaciology*, 42, 59–66. <https://doi.org/10.3189/172756405781813087>

- 677 Price, M. F. (1992). Patterns of the development of tourism in mountain environments.
678 *GeoJournal*, 27(1), 87-96.
- 679 Ramsankaran, R., Pandit, A., & Azam, M. F. (2018). Spatially distributed ice-thickness
680 modelling for Chhota Shigri Glacier in western Himalayas, India. *International Journal of*
681 *Remote Sensing*, 39(10), 3320–3343. <https://doi.org/10.1080/01431161.2018.1441563>
- 682 Salzmann, N., Huggel, C., Rohrer, M., Silverio, W., Mark, B. G., Burns, P., & Portocarrero, C.
683 (2013). Glacier changes and climate trends derived from multiple sources in the data scarce
684 Cordillera Vilcanota region, southern Peruvian Andes. *The Cryosphere*, 7(1), 103–118.
685 <https://doi.org/10.5194/tc-7-103-2013>
- 686 Sam, L., Kumar, R., & Bhardwaj, A. (2019). Climate and Remotely Sensed Markers of Glacier
687 Changes in the Himalaya. In *Environmental Change in the Himalayan Region* (pp. 65-88).
688 Springer, Cham.
- 689 Schmidt, S., & Nüsser, M. (2017). Changes of High Altitude Glaciers in the Trans-Himalaya
690 of Ladakh over the Past Five Decades (1969–2016). *Geosciences*, 7(2), 27.
691 <https://doi.org/10.3390/geosciences7020027>
- 692 Schmidt, S., Nüsser, M., Baghel, R., & Dame, J. (2020). Cryosphere hazards in Ladakh: The
693 2014 Gya glacial lake outburst flood and its implications for risk assessment. *Natural Hazards*,
694 104(3), 2071–2095. <https://doi.org/10.1007/s11069-020-04262-8>
- 695 Sen, P. K.: Estimates of the regression coefficient based on Kendall's Tau, *Am. Stat. J.*, 63,
696 1379–1389, <https://doi.org/10.2307/2285891>, 1968.
- 697 Shrestha, M., Acharya, S. C., & Shrestha, P. K. (2017). Bias correction of climate models for
698 hydrological modelling – are simple methods still useful? *Meteorol. Appl.*, 9.

- 699 Shukla, A., & Garg, P. K. (2019). Evolution of a debris-covered glacier in the western
700 Himalaya during the last four decades (1971–2016): A multiparametric assessment using
701 remote sensing and field observations. *Geomorphology*, 341, 1–14.
702 <https://doi.org/10.1016/j.geomorph.2019.05.009>
- 703 Shukla, A., Garg, S., Mehta, M., Kumar, V., & Shukla, U. K. (2020). Temporal inventory of
704 glaciers in the Suru sub-basin, western Himalaya: Impacts of regional climate variability. *Earth
705 System Science Data*, 12(2), 1245–1265. <https://doi.org/10.5194/essd-12-1245-2020>
- 706 Smith, S. (2012). Intimate geopolitics: Religion, marriage, and reproductive bodies in Leh,
707 Ladakh. *Annals of the Association of American Geographers*, 102(6), 1511-1528.
- 708 Soheb, M., Ramanathan, A., Angchuk, T., Mandal, A., Kumar, N., & Lotus, S. (2020). Mass-
709 balance observation, reconstruction and sensitivity of Stok glacier, Ladakh region, India,
710 between 1978 and 2019. *Journal of Glaciology*, 66(258), 627–642.
711 <https://doi.org/10.1017/jog.2020.34>
- 712 Stevens, S. (2003). Tourism and deforestation in the Mt Everest region of Nepal. *Geographical
713 Journal*, 169(3), 255-277.
- 714 Teutschbein, C., & Seibert, J. (2013). Is bias correction of regional climate model (RCM)
715 simulations possible for non-stationary conditions? *Hydrology and Earth System Sciences*,
716 17(12), 5061–5077. <https://doi.org/10.5194/hess-17-5061-2013>
- 717 Tian, L. et al. Two glaciers collapse in western Tibet. *Journal of Glaciology* 63, 194-197,
718 [doi:10.1017/jog.2016.122](https://doi.org/10.1017/jog.2016.122) (2017).
- 719 Warikoo, K. (2020). Ladakh: India's Gateway to Central Asia. *Strategic Analysis*, 44(3), 177-
720 192.

721 Table 1: Presents the data used in the present study.

	Data	Scene ID	Years	Spatial res.	Use
1	Landsat TM Landsat TM Landsat TM Landsat OLI	LT05_L1TP_147037_19910828_20170126_01_T1 LT05_L1TP_147037_19980916_20161222_01_T1 LT05_L1TP_147037_20100917_20161013_01_T1 LC08_L1TP_147037_20190910_20190917_01_T1	1991, 1998, 2010, 2019	30m	Glacier mapping
2	Corona	DS1107-1104DA015 (30 July) DS1107-1104DA016 (30 July) DS1107-1104DA017 (30 July) DS1107-1104DA018 (30 July) DS1107-1104DA019 (30 July) DS1107-1104DA020 (30 July)	1969	3m	Glacier, vegetation, built-up and water body mapping
3	ASTER DEM	AST14DMO.003:2025691837 (08 September) AST14DMO.003:2025691835 (08 September) AST14DMO.003:2404575282 (20 September) AST14DMO.003:2404575284 (20 September)	2004 2004 2020 2020	30m	Glacier thickness estimation, catchment delineation.
4	PlanetScope	20180829_045714_of2a, 20180829_045715_of2a, 20180829_045716_of2a, 20180829_045717_of2a, 20180829_045718_of2a, 20180829_045719_of2a, 20180829_045720_of2a, 20180829_045721_of2a, 20180829_045722_of2a, 20180829_045723_of2a, 20180829_045724_of2a, 20180829_045725_of2a, 20180829_045726_of2a, 20180829_050228_103b, 20180829_050229_103b, 20180829_050230_103b, 20180829_050231_103b, 20180829_050232_103b, 20180829_050233_103b, 20180829_050308_103d, 20180829_050309_103d, 20180829_050310_103d, 20180829_050311_103d, 20180829_050312_103d, 20180829_050313_103d, 20180829_050314_103d, 20180829_050315_103d, 20180829_050316_103d, 20180829_050317_103d, 20180829_050318_103d, 20180829_050319_103d, 20180829_050420_of17, 20180829_050421_of17, 20180829_050422_of17, 20180829_050424_of17, 20180829_050425_of17, 20180829_050426_of17, 20180829_050427_of17, 20180829_050428_of17, 20180829_050429_of17, 20180829_050532_of28, 20180829_050533_of28, 20180829_050534_of28, 20180829_050535_of28	2018	3m	Glacier, vegetation, built-up and water body mapping
5	ERA5 data	ERA5 hourly data on single levels from 1979 to 2019. DOI: 10.24381/cds.adbb2d47	1979- 2019	0.25°	Climate analysis
6	Census data	Census report of 1971, 1981, 2001 and 2011.	1971, 1981, 2001, 2011	10 year	Demographic change

722

723

724

725 Table 2: Results of Mann -Kendall and Sen's slope estimator for annual, JJAS and winter
 726 temperature and precipitation.

ERA5 points	Grid	ANNUAL				JJAS				WINTER			
		Mann-Kendall Significance (p)	Sens Slope (β)	Long-term Mean (°C or mm)	Change (°C or mm)	Mann-Kendall Significance (p)	Sens Slope (β)	Long-term Mean (°C or mm)	Change °C or mm	Mann-Kendall Significance (p)	Sens Slope (β)	Long-term Mean (°C or mm)	Change °C or mm
Leh Temperature		0.01	0.04	7.65	0.21	0.01	0.05	18.67	0.11	0.05	0.03	-0.45	-2.73
Leh Precipitation		0.4	-0.33	58.12	-0.23	0.6	-0.1	27.65	-0.15	0.9	0.001	19.27	0.00

727

728

729

730

731

732

733

734

735

736

737

738

739

740

741

742 Table 3: Uncertainty in glacierised area for different years through buffer based assessment.

Region	1969	1991	1998	2010	2019
	<i>km²</i>	<i>km²</i>	<i>km²</i>	<i>km²</i>	<i>km²</i>
Stok	±0.1 (0.8%)	±0.6 (6.1%)	±0.6 (6.1%)	±0.6 (6.6%)	±0.6 (7.1%)
Kang Yatze	±0.5 (0.7%)	±3.4 (4.9%)	±3.3 (5.0%)	±3.2 (5.4%)	±3.1 (5.6%)
All	±0.6 (0.5%)	±4 (3.9%)	±3.9 (4.0%)	±3.8 (4.1%)	±3.7 (4.2%)

743

744

745

746

747

748

749

750

751

752

753

754

755

756

757

758

759 Table 4: Estimated uncertainty in mean thickness (m) and total ice volumes (km³) in Glatop2,
 760 slope dependent and area scaling methods.

Uncertainties in glabtop2 and slope dependent methods								
REGIO N	2004				2020			
	Thickness		Volume		Thickness		Volume	
	m		km ³		m		km ³	
Stok	±4.6 (±23.7%)		±0.002 (±23.8%)		±3.8 (±22.6%)		±0.002 (±22.6%)	
Kang Yatze	±6.4 (±25.5%)		±0.009 (±25.7%)		±4.9 (±23%)		±0.006 (±23.1%)	
All	±6 (±25.1%)		±0.007 (±25.3%)		±4.63 (±23%)		±0.005 (±22.9%)	
Uncertainties in area scaling method								
REGION	2004				2020			
	Glacier area +5%		Glacier area -5%		Glacier area +5%		Glacier area -5%	
	Chen and Ohmura (1990)	Bahr et al., (1997)	Chen and Ohmura (1990)	Bahr et al., (1997)	Chen and Ohmura (1990)	Bahr et al., (1997)	Chen and Ohmura (1990)	Bahr et al., (1997)
	km ³ (Difference)	km ³ (Difference)	km ³ (Difference)	km ³ (Difference)	km ³ (Difference)	km ³ (Difference)	km ³ (Difference)	km ³ (Difference)
Stok	0.31 (+6.9%)	0.35 (+6.1%)	0.27 (-6.9%)	0.31 (-6.1%)	0.27 (+8.0%)	0.3 (+7.1%)	0.23 (-8.0%)	0.26 (-7.1%)
Kang Yatze	3.08 (+6.9%)	3.55 (+6.9%)	2.69 (-6.6%)	3.09 (-6.9%)	2.85 (+6.7%)	3.29 (+7.2%)	2.5 (-6.4%)	2.87 (-6.5%)
All	3.39 (+6.9%)	3.9 (+6.8%)	2.96 (-6.6%)	3.4 (-6.8%)	3.12 (+6.8%)	3.59 (+7.2%)	2.73 (-6.5%)	3.13 (-6.6%)

761

762

763

764

765

766

767

768

769

770 Table 5: Uncertainty in lake and build up area, and accuracy assessment for vegetation area.

Uncertainties in the lake area								
REGION	Analyst A		Analyst B		Analyst C		±Uncertainty (%)	
	<i>1969 (km2)</i>	<i>2018 (km2)</i>	<i>1969 (km2)</i>	<i>2018 (km2)</i>	<i>1969 (km2)</i>	<i>2018 (km2)</i>	<i>1969</i>	<i>2018</i>
Stok Region	0.009	0.022	0.009	0.021	0.008	0.023	2.35	2.61
Kang Yatze Region	0.237	0.524	0.231	0.511	0.239	0.523	1.33	1.17
All	0.246	0.546	0.240	0.532	0.247	0.546	1.21	1.22
Uncertainties in the build-up area								
SAMPLE VILLAGE	<i>1969 (m2)</i>	<i>2018 (m2)</i>	<i>1969 (m2)</i>	<i>2018 (m2)</i>	<i>1969 (m2)</i>	<i>2018 (m2)</i>	<i>1969</i>	<i>2018</i>
Chuchot Village	0.280	0.969	0.264	0.939	0.273	0.989	2.28	2.12
Stok Village	0.062	0.492	0.061	0.517	0.064	0.501	1.91	2.08
All	0.342	1.461	0.325	1.456	0.337	1.490	2.06	1.04
Accutacy assessment for the vegetation area								
REGION	<i>1969</i>				<i>2018</i>			
	<i>Overall Accuracy</i>		<i>Kappa Cofficient</i>		<i>Overall Accuracy</i>		<i>Kappa Cofficient</i>	
Stok	79%		0.72		92%		0.9	
Kang Yatze	74%		0.6		89%		0.86	
All	77%		0.66		91%		0.88	

771

772

773

774

775

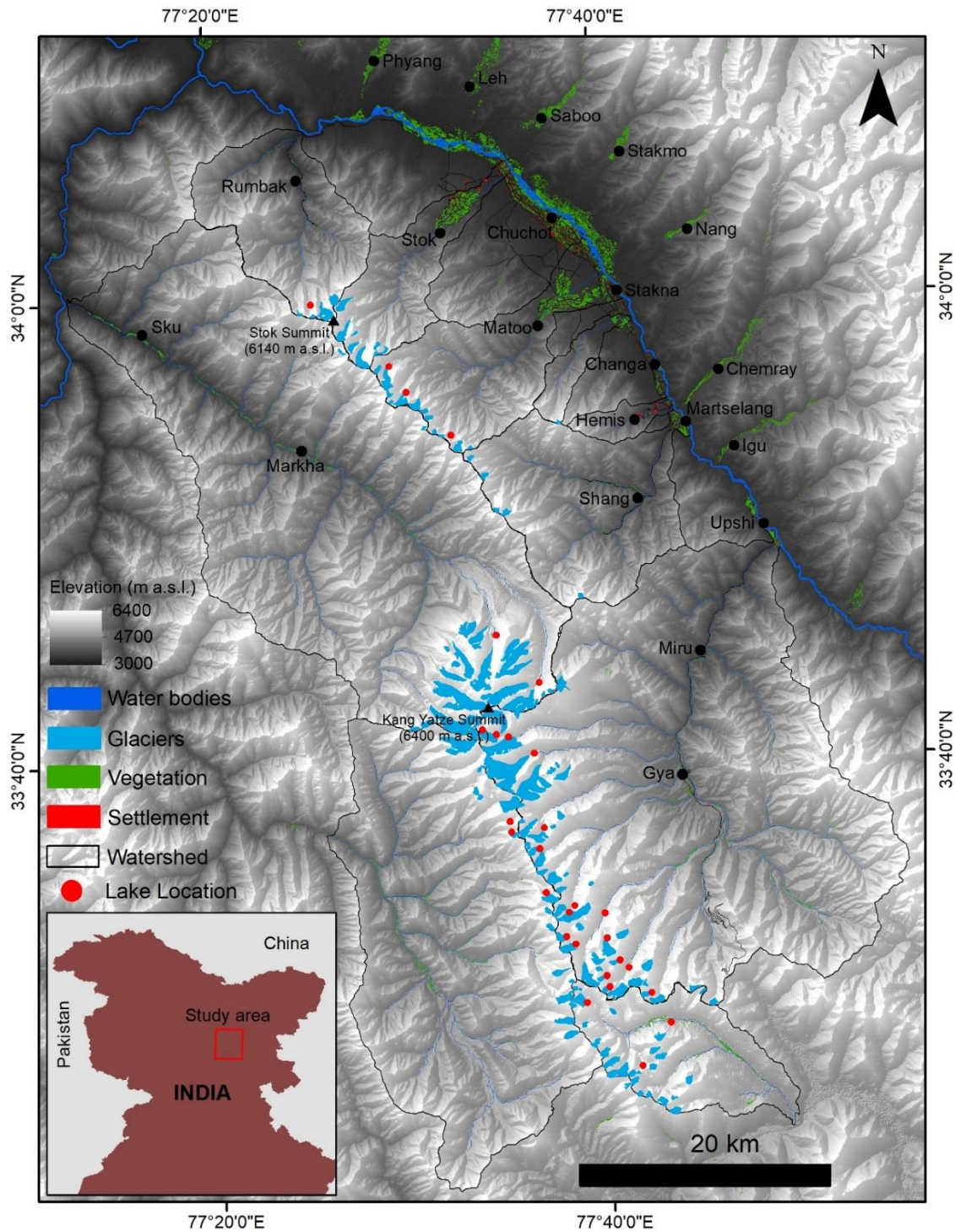
776

777

778

779

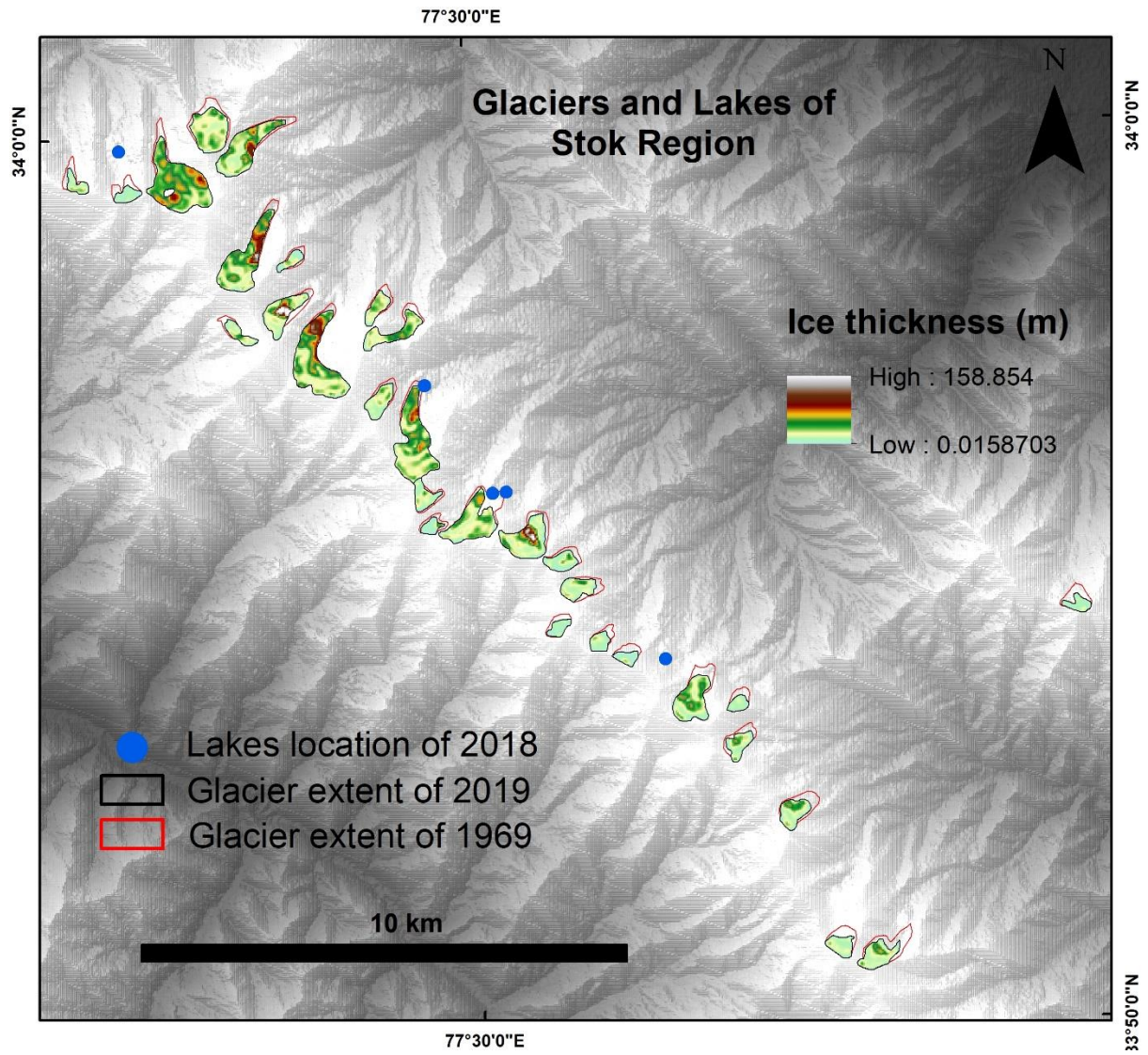
780



781

782 **Figure 1:** Location map of the study area presenting all the mapped key environmental
 783 parameters. Advanced Spaceborne Thermal Emission and Reflection Radiometer Digital
 784 Elevation Model (ASTER DEM) has been used in the background to provide the topographic
 785 details. The inset map highlights the contextual location of study area in North India.

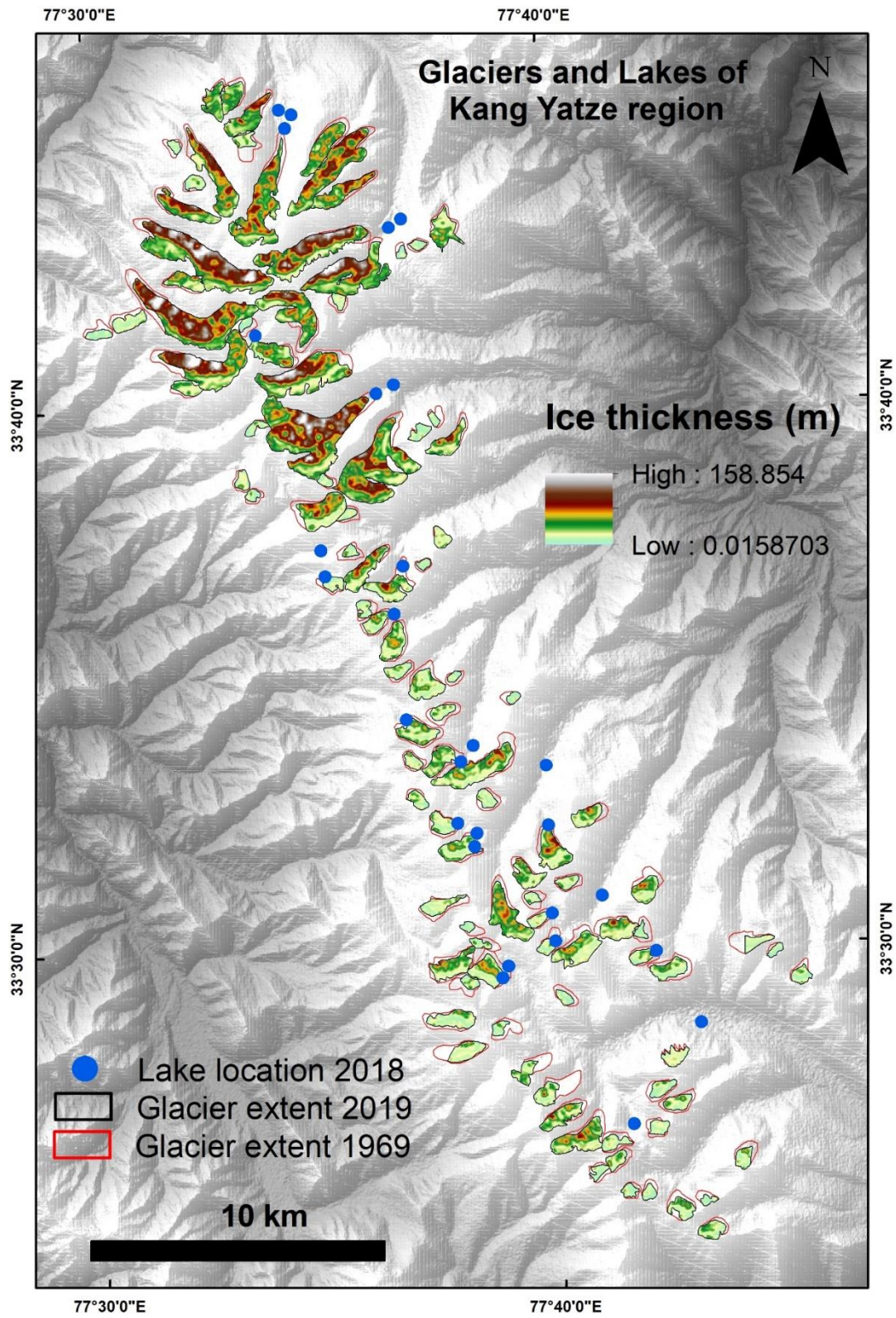
786



787

788 **Figure 2:** Presents the glacier outlines of 1969 and 2019, glacier thickness of 2020 and location
789 of lakes in Stok region

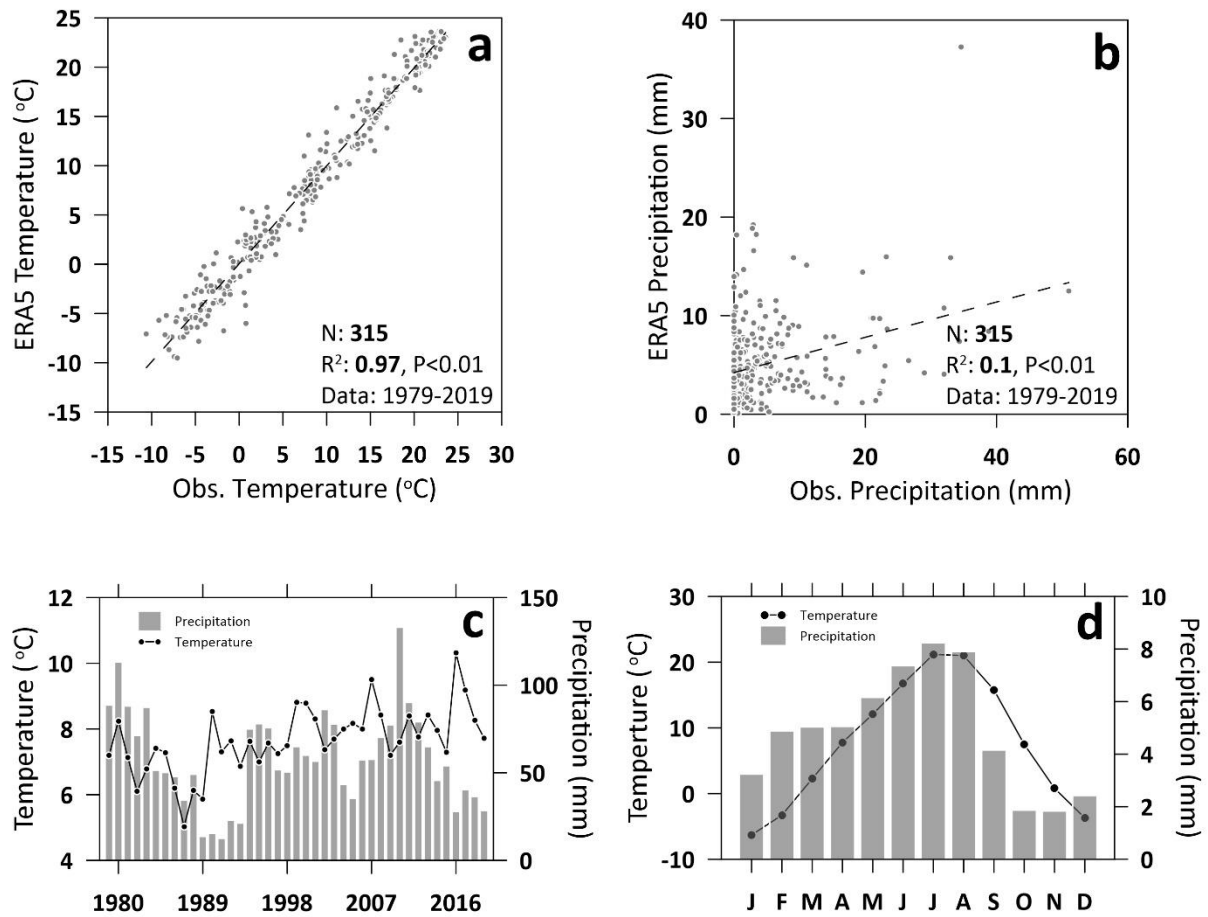
790



791

792 **Figure 3:** Presents the glacier outlines of 1969 and 2019, glacier thickness of 2020 and location
793 of lakes in Kang Yatze region

794



795

796 **Figure 4:** ERA5 bias corrected temperature and precipitation of Leh grid from 1979 to 2019.

797 a and b are the correlation between observed and ERA5 reanalysis temperature and

798 precipitation. c and d are annual and monthly temperature and precipitation.

799

800

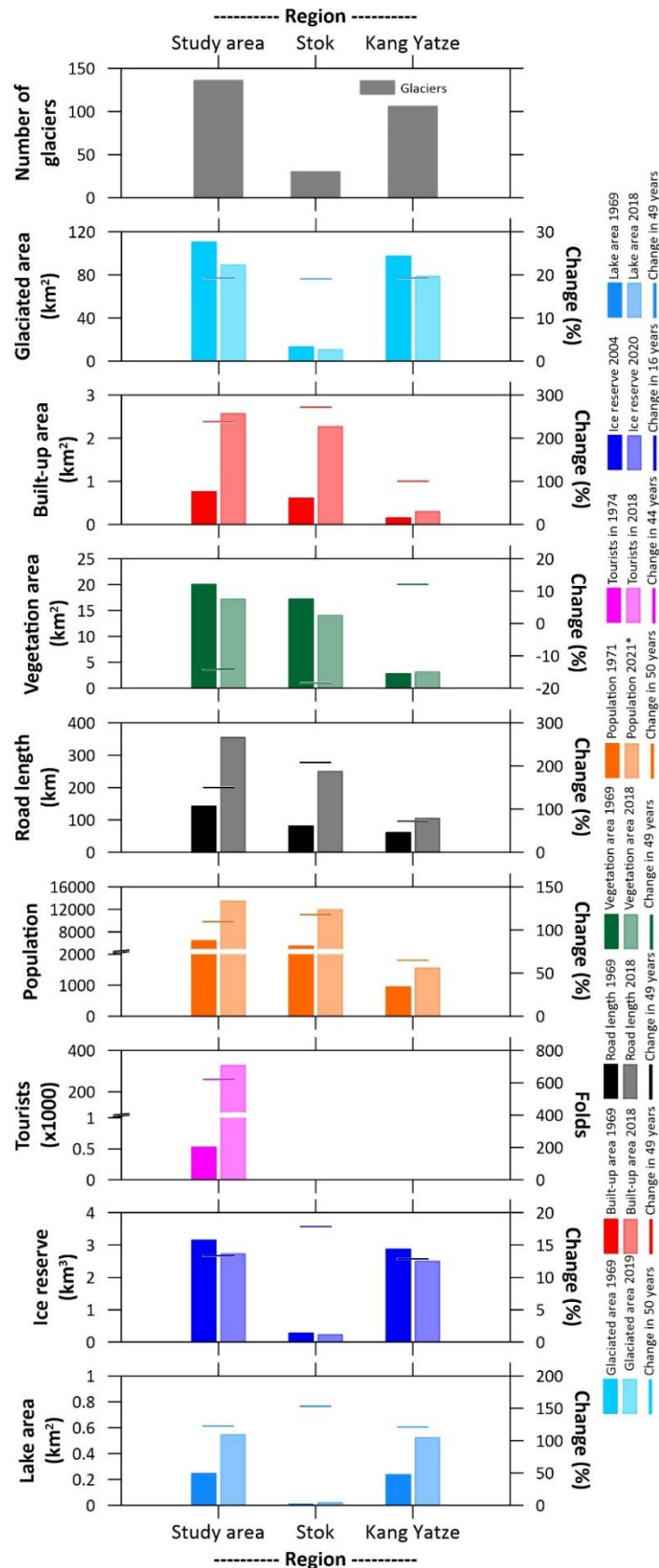
801

802

803

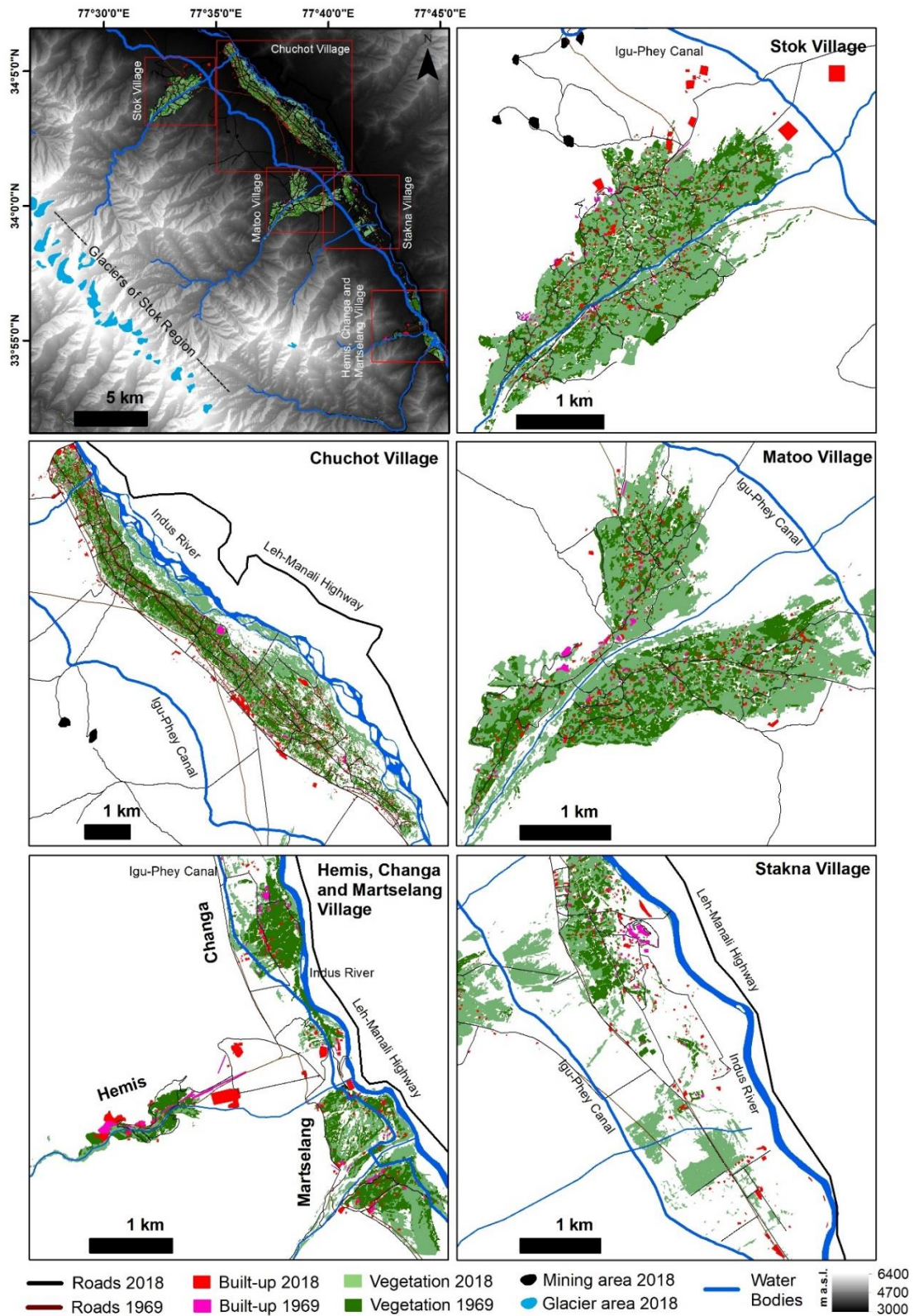
804

805



806

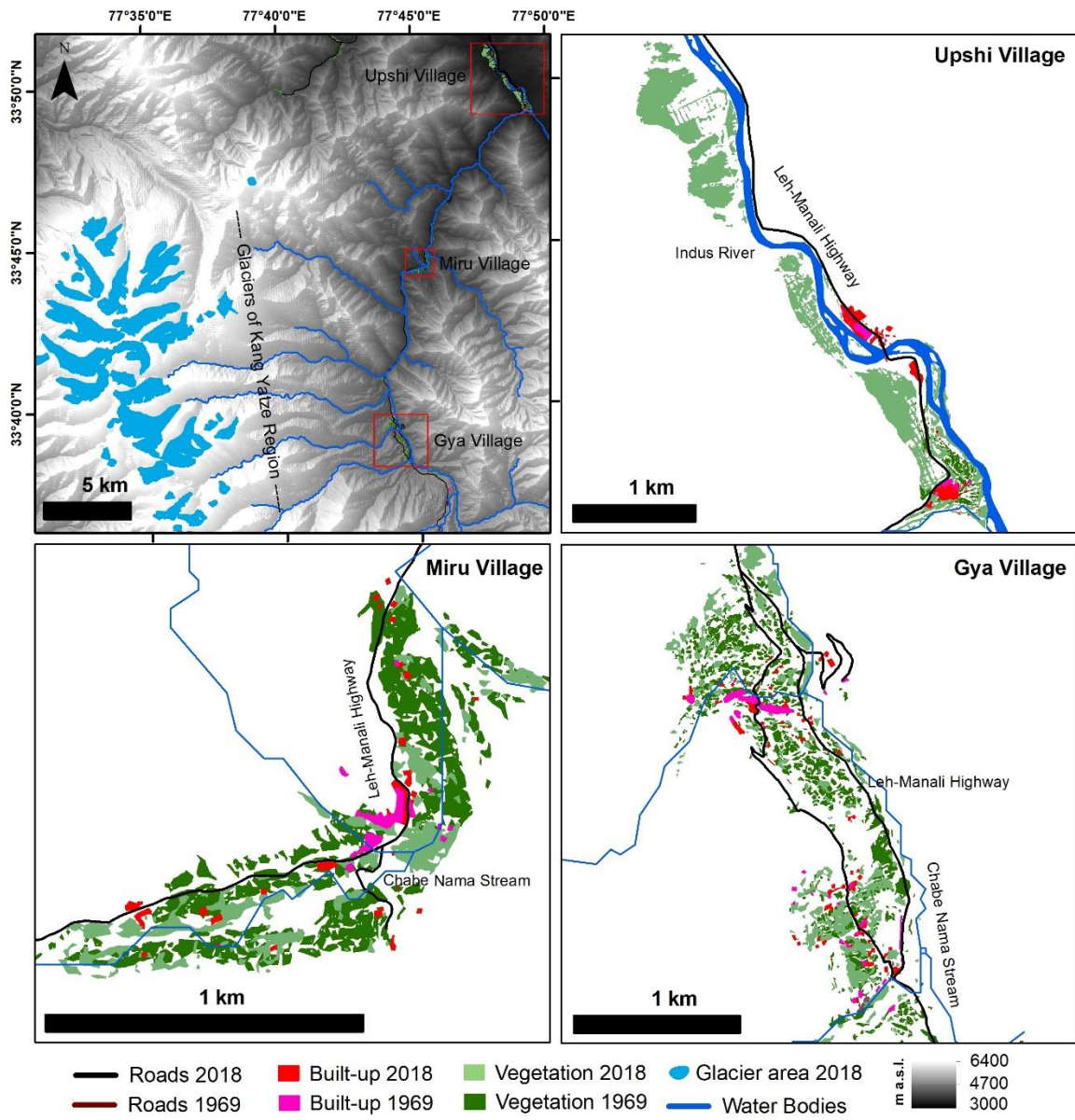
807 **Figure 5:** Total change of key environmental parameters over the years in the study area, Stok
 808 and Kang Yatze regions



809

810 **Figure 6:** Presents Vegetation, Built-up and Waterbodies map over the years in Stok region.

811



812

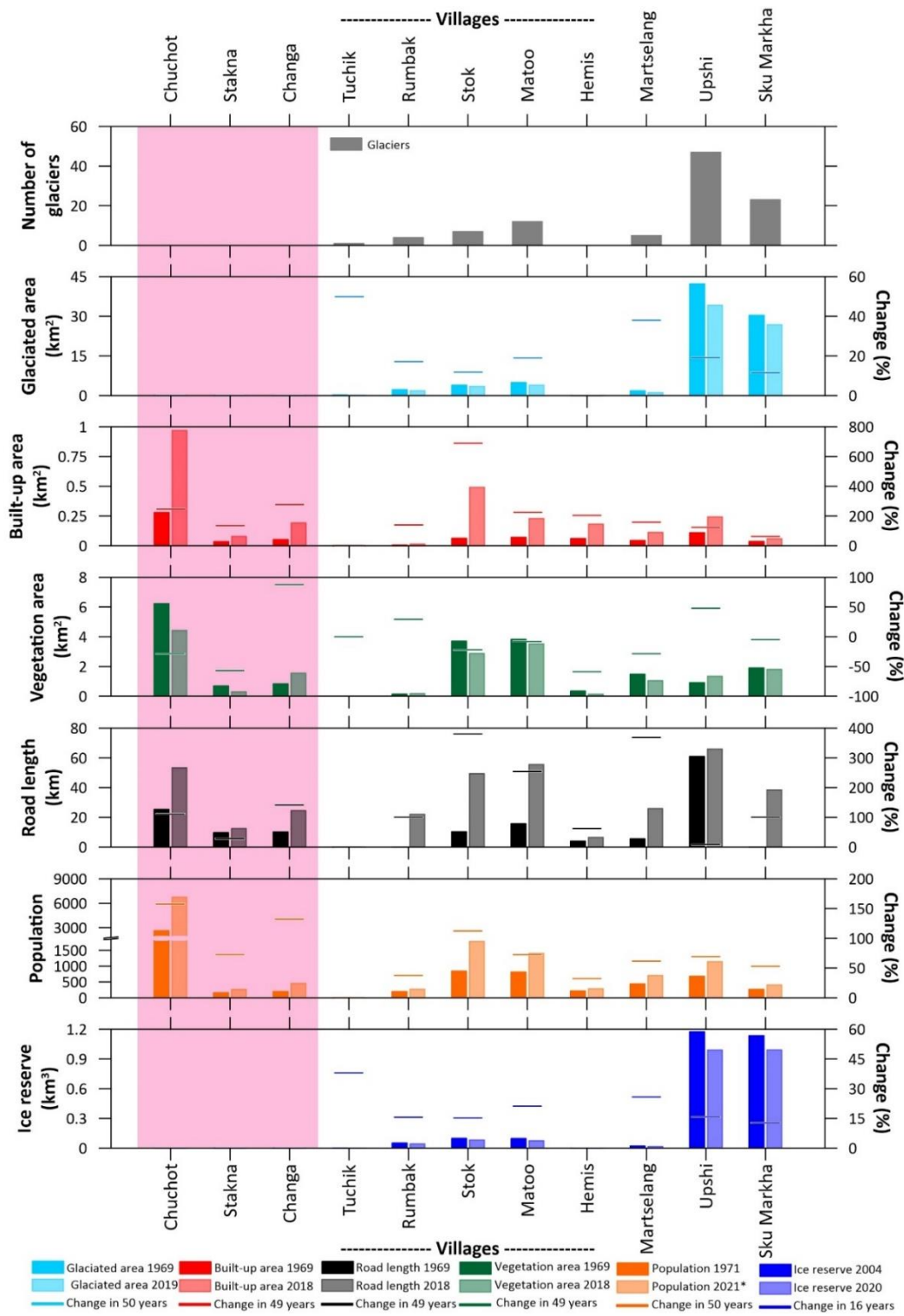
813 **Figure 7:** Presents Vegetation, Built-up and Waterbodies map over the years in Kang Yatze
 814 region

815

816

817

818



819

820 **Figure 8:** Village level change of key environmental parameters over the years in the study
 821 area. The section with pink background represents the Indus-fed villages

822

823

824

825 **Figure 9:** Location map of the study area presenting all the mapped key environmental
826 parameters. Advanced Spaceborne Thermal Emission and Reflection Radiometer Digital
827 Elevation Model (ASTER DEM) has been used in the background to provide the topographic
828 details. The inset map highlights the contextual location of study area in North India.

829 **Figure 10:** Presents the glacier outlines of 1969 and 2019, glacier thickness of 2020 and
830 location of lakes in Stok region

831 **Figure 11:** Presents the glacier outlines of 1969 and 2019, glacier thickness of 2020 and
832 location of lakes in Kang Yatze region

833 **Figure 12:** ERA5 bias corrected temperature and precipitation of Leh grid from 1979 to 2019.
834 a and b are the correlation between observed and ERA5 reanalysis temperature and
835 precipitation. c and d are annual and monthly temperature and precipitation.

836 **Figure 13:** Total change of key environmental parameters over the years in the study area,
837 Stok and Kang Yatze regions

838 **Figure 14:** Presents Vegetation, Built-up and Waterbodies map over the years in Stok region.

839 **Figure 15:** Presents Vegetation, Built-up and Waterbodies map over the years in Kang Yatze
840 region

841 **Figure 16:** Village level change of key environmental parameters over the years in the study
842 area. The section with pink background represents the Indus-fed villages